J Mater Sci (2016) 51:7300–7308

Effects of the composition of diffusion source on the surface concentration and effective surface diffusivity of Zn in n-GaSb

Hong Ye[1,*] and Qing Ni[1]

[1] *Department of Thermal Science and Energy Engineering, University of Science and Technology of China, Hefei 230027, People's Republic of China*

Received: 8 March 2016
Accepted: 23 April 2016
Published online: 3 May 2016

ABSTRACT

Understanding the Zn diffusion behavior in GaSb is very important to accurately control the distribution of Zn during the fabrication of photoelectric devices. The surface concentration and effective surface diffusivity are two key parameters for modeling the Zn profile in GaSb. The experimental results indicated that when the diffusion temperature and time are kept unchanged, the diffusion profiles with pure Zn, Zn–Sb, and Zn–Ga sources differ in the surface concentration and effective surface diffusivity. To quantitatively explain the effects of source composition on the two parameters, the relationship between the two parameters and the vapor pressure surrounding the GaSb wafer in the diffusion process was deduced based on a surface-equilibrium assumption and the substitutional-interstitial mechanism. The Ga/Sb/Zn ternary phase diagram was calculated and discussed for determining the vapor pressures in different source cases. The ratio of surface concentrations and that of effective surface diffusivities between different sources were obtained to quantitatively explain the experiment results. The theoretical and experimental results both indicated that adding Sb to pure Zn source keeps the surface concentration unchanged while slightly decreases the effective surface diffusivity, and that adding Ga to pure Zn source significantly decreases both the surface concentration and effective surface diffusivity.

Introduction

With a bandgap of 0.72 eV at room temperature, GaSb is a promising material for fabricating optoelectronic and electronic devices with a response spectrum in the near infrared wavelength, such as lasers [1, 2], photodiode [3, 4], thermophotovoltaic cells [5, 6], and so on. The key structure of these devices is the p–n junction, which can be fabricated by diffusing Zn into an n-GaSb substrate. Because Zn profile in GaSb after diffusion exerts a significant influence on the performance of the devices, it is

Address correspondence to E-mail: hye@ustc.edu.cn

DOI 10.1007/s10853-016-0012-7

necessary to understand the diffusion mechanism of Zn in GaSb to strictly control the diffusion process. In the past four decades, a great deal of work has been carried out studying the diffusion of Zn into GaSb [7–17]. According to the published work, the boundary condition at the wafer surface plays a key role in modeling the Zn concentration profiles. Some researchers, e.g., Sunder et al. [15] and Tuck and Jay [18], assumed that the surface of the GaSb wafer was in an equilibrium state during the diffusion process. However, a detailed discussion on the surface diffusion parameters is still lacking. During the Zn diffusion process, many Sb atoms evaporate from the GaSb surface making the wafer not stoichiometric. To suppress the process, Sb was added to the diffusion source to maintain a saturated Sb vapor pressure [7, 9, 10, 13]. Conibeer et al. [9] found that adding Sb to Zn source can shorten the p–n junction depth by decreasing the diffusivity because that Zn diffusivity is inversely proportional to the Sb vapor pressure. Similar results have been reported in GaAs [19], GaP [18], and InP [20, 21]. In addition to Zn and Zn–Sb sources, Zn–Ga was often used as a diffusion source [8, 12]. So far, few investigations have been reported on a quantitative analysis of the effects of the source composition on the surface diffusion parameters of Zn in GaSb.

This work aimed to quantitatively analyze the effects of the source composition on the surface diffusion parameters based on a surface-equilibrium assumption, to determine the boundary conditions for predicting the Zn diffusion profiles in the future. Based on the substitutional–interstitial mechanism, the relationship between the surface diffusion parameters and the vapor pressure were deduced. Then the vapor pressures were calculated according to Ga/Sb/Zn ternary phase diagram.

Materials and methods

Tellurium-doped ($n = 4 \times 10^{17}$ cm^{-3}), ⟨100⟩-oriented GaSb substrates made by the Institute of Semiconductors (Chinese Academy of Sciences) were used in the experiments. The GaSb samples were all 1 cm × 1 cm × 500 μm in size. The diffusion sources were pure Zn, Zn–Sb with 45 wt% Zn and Zn–Ga with 3 wt% Zn, respectively. The diffusion experiments were performed in a pseudo-closed graphite box for pure Zn and Zn–Sb sources, while in a closed ampoule for Zn–Ga source. The diffusion temperature and time are 500 °C and 2 h, respectively. The diffusion sources were all sufficient to maintain the pressures of Zn, Sb, and Ga saturated during the diffusion process. After diffusion, the Zn concentration profiles were obtained using a secondary ion mass spectrometry (SIMS). The details of the experiments were described in our recent publication [17].

Results and discussion

Experimental results

The inset of Fig. 1 shows the SIMS profiles of Zn concentration after diffusion at 500 °C for 2 h using different diffusion sources. The yellow solid line represents the doping concentration of Te in GaSb, i.e., 4×10^{17} cm^{-3}. The intersections of the Zn profiles and Te profile represent the junction depths. The SIMS measurement was carried out in Evans Analytical Group® (EAG). Because of the surface contamination caused by coating GaSb wafer with gold, as well as the surface transient effect caused by the unequilibrium between the primary ions and sputtered secondary ions in the beginning, the Zn concentration within at least 0.015 μm is not reliable. Besides, Bett et al. [10] and Serreze and Marek [22] considered that the concentration in the surface layer region within 0.1 μm was not reliable and can be omitted in their analysis. As a compromise, we consider that the SIMS measurement in the surface layer region within 0.05 μm is not highly reliable. Thus the region within 0.05 μm will be neglected in the following analysis. Moreover, the part at the very end of SIMS profile which is beyond the measurement accuracy will also be disregarded. Thus, the Zn concentration profiles retained for further analysis are shown in Fig. 1. It can be seen that Zn diffusion profile exhibits kink-and-tail shape when using pure Zn or Zn–Sb source, while exhibits box shape for Zn–Ga source. If compared with the profile for pure Zn source, adding Sb to pure Zn source shortens the junction depth but holds the profile shape and surface concentration, while adding Ga to pure Zn source can significantly decrease the junction depth and surface concentration, and change the profile from a kink-and-tail one into a box one.

Substitutional–interstitial mechanism has been widely accepted for explaining the diffusion behavior

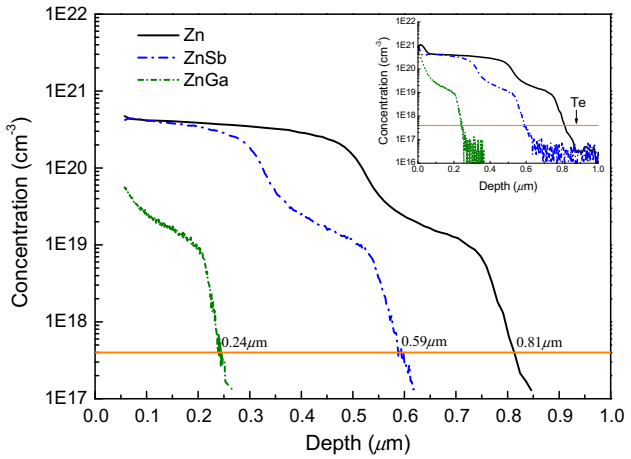

Figure 1 SIMS profiles of Zn concentration using pure Zn, Zn–Sb, and Zn–Ga sources. The diffusion temperature and time are 500 °C and 2 h, respectively. The *inset* represents the original SIMS profile.

of Zn in III–V compound semiconductors. It assumes that Zn atoms exist substitutionally on gallium sites (Zn_{Ga}) or interstitially (Zn_i) among the interstitial sites. The solubility of Zn_{Ga} is much greater than that of Zn_i, while the diffusivity of Zn_{Ga} is much smaller that of Zn_i. The interchange between Zn_i and Zn_{Ga} is governed by the dissociative mechanism [23] or the kick out mechanism [24]. Our recent publication [17] indicated that Zn diffusion is governed by the dissociative mechanism in the surface layer region:

$$Zn_i^+ + V_{Ga} \underset{k_2}{\overset{k_1}{\rightleftarrows}} Zn_{Ga}^- + 2h^+, \tag{1}$$

where k_1 and k_2 are the forward and reverse reaction constants, respectively. The time variations of Zn_i^+ and Zn_{Ga}^- concentrations can be written as [25]

$$\frac{\partial C_i}{\partial t} = D_i \frac{\partial^2 C_i}{\partial x^2} - k_1 C_{V_{Ga}} C_i + k_2 C_s p^2 \tag{2}$$

$$\frac{\partial C_s}{\partial t} = D_s \frac{\partial^2 C_s}{\partial x^2} + k_1 C_{V_{Ga}} C_i - k_2 C_s p^2, \tag{3}$$

where C_i, $C_{V_{Ga}}$, C_s, and p are the concentrations of Zn_i, V_{Ga}, Zn_{Ga}, and hole, respectively, D_i and D_s are the diffusivities of Zn_i and Zn_{Ga}, respectively, t is the diffusion time, x is the distance from the surface of the wafer. It is assumed that the surface layer region of the GaSb wafer is in an equilibrium state. Thus, the concentration of Zn_i is in equilibrium with that of Zn_{Ga}, and we have $k_1 C_{V_{Ga}} C_i = k_2 C_s p^2$ [25]. The time variation of the total Zn atom concentration ($C = C_i + C_s \cong C_s$) can be expressed as

$$\frac{\partial (C_i + C_s)}{\partial t} = \frac{\partial}{\partial x}\left(D_i \frac{\partial C_i}{\partial x} + D_s \frac{\partial C_s}{\partial x} \right). \tag{4}$$

An effective diffusivity D can be defined as

$$D = D_i \frac{\partial C_i}{\partial C} + D_s \frac{\partial C_s}{\partial C}. \tag{5}$$

As $D_i(\partial C_i/\partial C) \gg D_s(\partial C_s/\partial C)$, the effective diffusivity can be reduced to

$$D = D_i \frac{\partial C_i}{\partial C}. \tag{6}$$

Thus, Eq. (4) is simplified to

$$\frac{\partial C}{\partial t} = \frac{\partial}{\partial x}\left(D \frac{\partial C}{\partial x} \right). \tag{7}$$

According to the Boltzmann–Matano method [25], a new variable $\eta = x/\sqrt{t}$ is substituted into Eq. (7), and it can be simplified and integrated to establish the relationship between the effective diffusivity and the Zn concentration:

$$D = -\frac{1}{2t} \frac{\int_0^{C_x} x \mathrm{d}C}{(\mathrm{d}C/\mathrm{d}x)_{C_x}}, \tag{8}$$

where C_x is the Zn concentration at a depth of x. $\int_0^{C_x} x \mathrm{d}C$ is the area enclosed by the Zn concentration profile, $C = C_x$, $C = 0$, and the vertical axis in Fig. 1. $(\mathrm{d}C/\mathrm{d}x)_{C_x}$ is the slope at the point C_x. Tuck and Kadhim [26] observed a variation in profile shape with diffusion time of Zn in GaAs, and they indicated that the standard Boltzmann-Matano method is not strictly valid for this kind of profiles. Thus, the effective diffusivity obtained by Boltzmann analysis can only be considered as an approximate result. It is noteworthy that the lower limit of the integration in the Boltzmann analysis should be the minimum concentration in Fig. 1, i.e., 1.3×10^{17} cm^{-3}, which is close to 0. Table 1 gives the effective surface diffusivities for different diffusion sources by Boltzmann–Matano analysis, also given are the corresponding surface concentrations. It can be seen that when the diffusion temperature and duration are kept

Table 1 The surface concentration and effective surface diffusivity for different sources

Diffusion source	C_{sur}/cm^{-3}	D_{sur}/cm^2 s^{-1}
Zn	4.7×10^{20}	7.8×10^{-14}
Zn–Sb	4.2×10^{20}	6.8×10^{-14}
Zn–Ga	5.5×10^{19}	6.2×10^{-15}

unchanged, the composition of diffusion source exerts a great effect on the surface diffusion parameters. Adding Sb to pure Zn source does not change the surface concentration while slightly decreases the effective surface diffusivity, resulting in a slight decrease of the junction depth. Adding Ga to pure Zn source simultaneously decreases the surface concentration and effective surface diffusivity significantly, leading to a significant decrease of the junction depth. According to Conibeer et al. [9] and Shin et al. [27], the variation in the source composition will change the vapor pressure surrounding the wafer, and the variation in the vapor pressure will further alter the surface diffusion parameters. To quantitatively analyze the effects of the source composition on the surface concentration and effective surface diffusivity, the relationship between the two parameters and the vapor pressures surrounding the wafer will be deduced based on the substitutional–interstitial mechanism in the next section.

The effects of vapor pressures on the surface concentration and effective surface diffusivity

During the diffusion process, the saturated vapor formed by the diffusion sources is in a local equilibrium with GaSb surface layer region. Zn enters the GaSb wafer via the monatomic vapor phase to form Zn_i^+. According to the substitutional-interstitial mechanism, Zn_i^+ diffuses from the surface layer into the depth direction through dissociative or kick out mechanism. The species Zn_i^+ in the surface layer region is in equilibrium with the vapor phase Zn in the ambient [28]:

$$Zn_{vap} \rightleftarrows Zn_i^+ + e^-, \tag{9}$$

where Zn_{vap} is vapor phase Zn, e is electron. When using pure Zn as the diffusion source, more Sb atoms than Ga atoms evaporate from the wafer due to a lower boiling point. The Sb and Ga atoms in the surface layer region are in equilibrium with the Sb and Ga vapors surrounding the wafer, respectively:

$$Sb_{vap} + V_{Sb} \rightleftarrows Sb_{Sb} \tag{10}$$

$$Ga_{vap} + V_{Ga} \rightleftarrows Ga_{Ga}, \tag{11}$$

where Sb_{vap} and Ga_{vap} are Sb vapor and Ga vapor, respectively, V_{Sb} and V_{Ga} are Sb vacancy and Ga vacancy in the surface region, respectively, Sb_{Sb} and Ga_{Ga} are Sb and Ga atoms occupying their own positions, respectively. Moreover, the reaction between Ga vapor and Sb vapor can be described as

$$Ga_{vap} + Sb_{vap} \rightleftarrows GaSb. \tag{12}$$

Appling the law of mass action to Eqs. (9)–(12), we have

$$P_{Zn} = K_1 C_i n \tag{13}$$

$$P_{Sb} C_{V_{Sb}} = K_2 \tag{14}$$

$$P_{Ga} C_{V_{Ga}} = K_3 \tag{15}$$

$$P_{Ga} P_{Sb} = K_4, \tag{16}$$

where n, $C_{V_{Sb}}$, and $C_{V_{Ga}}$ are the concentrations of electrons, Sb vacancy and Ga vacancy, respectively, P_{Zn}, P_{Sb}, and P_{Ga} are the vapor pressures of Zn, Sb, and Ga, respectively, K_1, K_2, K_3, and K_4 are equilibrium constants. According to Eqs. (13)–(16),

$$C_i = P_{Zn}/K_1 n \tag{17}$$

$$C_{V_{Sb}} = K_2/P_{Sb} \tag{18}$$

$$C_{V_{Ga}} = (K_3/K_4)P_{Sb}. \tag{19}$$

It is seen from Eqs. (18) and (19) that the concentration of Sb vacancy in the surface region is inversely proportional to Sb vapor pressure surrounding the wafer, while the concentration of Ga vacancy in the surface region is proportional to Sb vapor pressure surrounding the wafer. When compared with the pure Zn source, using Zn–Sb source will increase the Sb vapor pressure but decrease the Ga vapor pressure. The former will suppress the evaporation of Sb atoms in the surface region, and hence decrease the concentration of Sb vacancy in this region. Inversely, the latter will enhance the evaporation of Ga atoms from the surface region, and increase the concentration of Ga vacancy in this region. The situation will be inverse when using Zn–Ga diffusion source.

Appling the law of mass action to Eq. (1), we have

$$C_i C_{V_{Ga}} = K_5 C_s p^2. \tag{20}$$

By substituting Eqs. (17) and (19) into Eq. (20), one can obtain

$$K_8 P_{Zn} P_{Sb} = C_s p^2 n, \tag{21}$$

where $K_8 = K_3/K_1 K_4 K_5$. In the semiconductors, the product of the concentration of hole (p) and that of electron (n) equals the square of the intrinsic carriers (n_i) [29]. Thus, Eq. (20) is rewritten as

$$K_8 P_{Zn} P_{Sb} = C_s p n_i^2. \quad (22)$$

In neutrality, $C_s \approx p$, one can obtain the expression of the surface concentration C_{sur}:

$$C_{sur} \cong (C_s)_{sur} = K_9 P_{Zn}^{1/2} P_{Sb}^{1/2} \quad (23)$$

where the subscript sur represents the surface and $K_9 = K_8^{1/2}/n_i$. It can be seen that C_{sur} is proportional to $P_{Zn}^{1/2} P_{Sb}^{1/2}$. According to Eq. (20), the effective surface diffusivity can be written as

$$D = D_i \frac{\partial C_i}{\partial C} = D_i \left(\frac{3K_5}{C_{V_{Ga}}} \right) C_s^2. \quad (24)$$

Substituting Eq. (19) into Eq. (24), one can obtain the effective surface diffusivity D_{sur}:

$$D_{sur} = D_i \left(\frac{3K_5 K_2}{K_3} \frac{1}{P_{Sb}} \right) (C_s)_{sur}^2 \cong D_i \left(\frac{3K_5 K_2}{K_3} \frac{1}{P_{Sb}} \right) C_{sur}^2. \quad (25)$$

It can be seen that D_{sur} is inversely proportional to the Sb vapor pressure surrounding the wafer and proportional to the square of the surface concentration.

Based on the above derivation, it can be claimed that the surface concentration of Zn in n-GaSb is in a relationship with the vapor pressures of Zn and Sb surrounding the wafer, while the effective surface diffusivity is in a relationship with the vapor pressure of Sb surrounding the wafer and the surface concentration. To validate the above derivation and quantitatively analyze the effects of the source composition on the surface diffusion parameters, one has to determine the concentration profile of Zn in GaSb and the vapor pressures of Sb and Zn surrounding the wafer. The former can be obtained by SIMS, while the latter can be obtained via the Ga/Sb/Zn ternary phase diagram.

The Ga/Sb/Zn phase diagram

The surface layer region of the GaSb wafer is in equilibrium with the vapor phase and liquid phase during the diffusion process and can be analyzed by a ternary equilibrium phase diagram. Based on the optimized thermodynamic parameters [30], the phase diagram of ternary Ga/Sb/Zn system was calculated by using the software package PANDAT 2014 Demo, which is based on modeling the Gibbs energies of all phases and minimizing the total Gibbs energy of the system. Figure 2 shows the isothermal section of the ternary Ga/Sb/Zn system at 500 °C. AB and BE are liquidus lines. L denotes the liquid phase region. Point C denotes the stoichiometric GaSb wafer. The regions related to this work are labeled I and II in Fig. 2, both of which contain solid GaSb and liquid phase. If a system can be represented by a point within region I, then it consists of solid GaSb, a liquid with composition given by the relevant point on the liquidus line AB and the vapor phase. There are three components and three phases, and the phase rule gives two degrees of freedom for this system. In our case, the diffusion temperature has been identified as 500 °C; there is only one independent variable, i.e., vapor pressure. Thus, the vapor pressure will vary as the system moves to another point within region I. If the system is within region II, there exists four phases: solid GaSb, solid compound composed of Sb and Zn, a liquid with composition given by point B, and the vapor phase. According to the phase rule there is only one degree of freedom in this system. Because the diffusion temperature has been identified as 500 °C, there is no independent variable. Thus, the systems represented by all points within region II have the same vapor pressure.

To obtain the vapor pressures of the components when using different diffusion sources, one has to determine the location of each diffusion system in the phase diagram. If stoichiometric GaSb wafer is heated at 500 °C without diffusion sources, more Sb

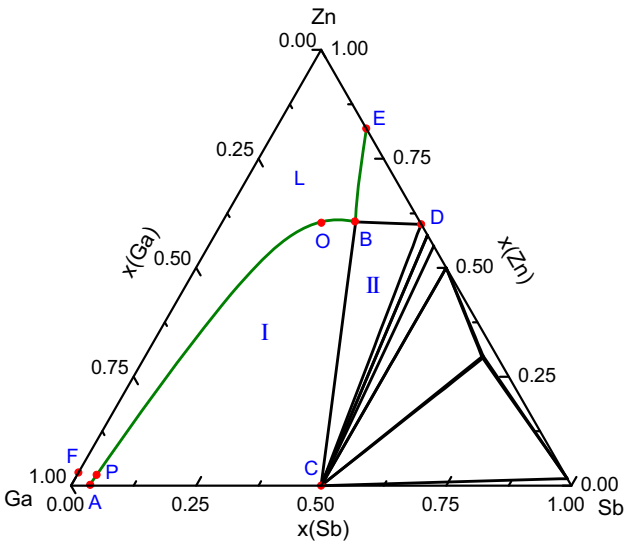

Figure 2 The isothermal section of ternary Ga/Sb/Zn system at 500 °C.

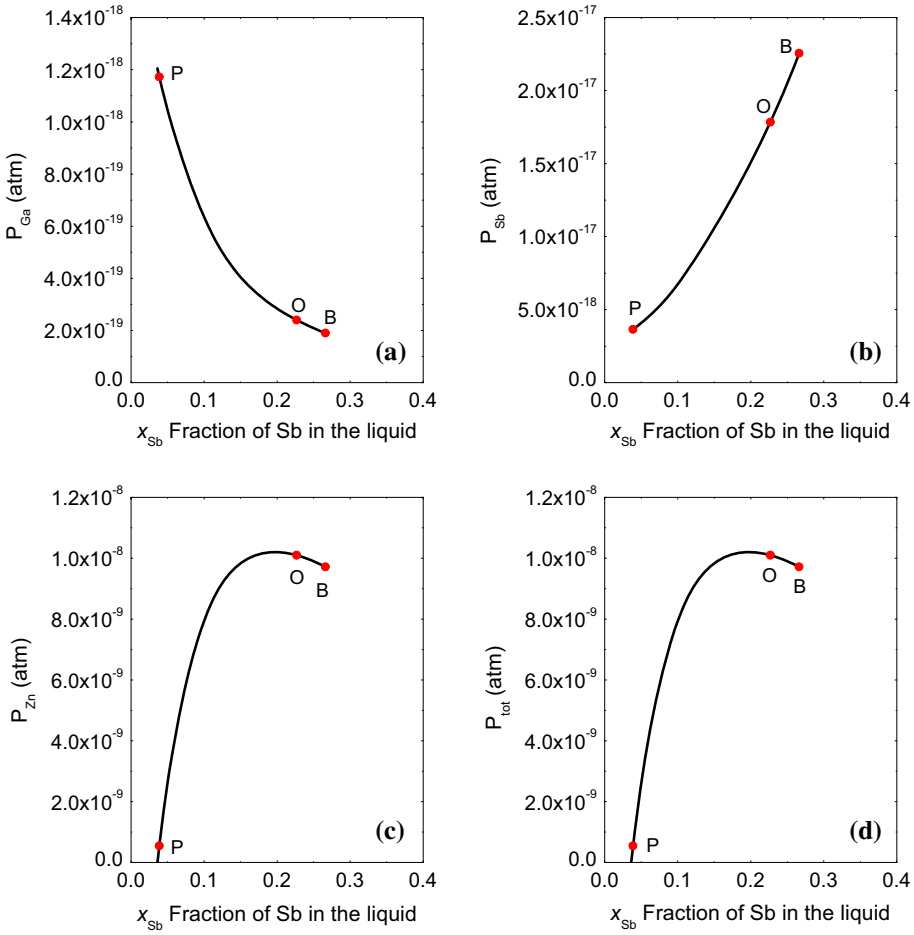

Figure 3 The vapor pressures as a function of the Sb fraction in the liquid phase along the liquidus line AB in Ga/Sb/Zn ternary phase diagram at 500 °C. **a**–**c** the vapor pressures of Ga, Sb, and Zn, respectively, **d** the total pressure of the system.

atoms than Ga atoms enter the vapor phase and the condensed phase becomes gallium-rich. The point representing the system moves in the direction C→A along the Ga–Sb base-line. If pure Zn source is added, the point moves off the Ga–Sb base-line and enters region I. And the composition of liquid phase can be given by a relevant point on the liquidus line AB. As the weight of pure Zn source increases, the liquid phase moves along A→O. When the liquid composition reaches point O (on the Zn–GaSb pseudobinary line), increasing the weight of Zn source no longer changes the liquid composition. If Sb is added to the sufficient pure Zn source, the liquid phase moves along O→B. Instead, if Ga is added, the liquid phase moves along O→A. Because the diffusion sources are sufficient in our experiments, the liquid phase compositions can be given by point O and B for pure Zn and Zn–Sb sources, respectively. For sufficient Zn–Ga sources, the liquid phase in the system can be estimated as the intersection point P at the liquidus line AB of the connection line between the Zn–Ga source represented by point F and GaSb wafer represented by point C [19]. In equilibrium state, the chemical potential of each component in any phase equals to that of this component in any other phase. According to the chemical potential of one component in liquid phase given by PANDAT, the chemical potential of this component in vapor phase can be calculated. Then the vapor pressure can be obtained. Figure 3 gives the vapor pressures along the liquidus line AB, where the horizontal axis x_{Sb} represents the Sb fraction in the liquid phase. Fig. 3a–c present the vapor pressures of Ga, Sb, and Zn, respectively, and Fig. 3d shows the total pressure of the system. As can be seen, the dominant component in the vapor phase surrounding the wafer is Zn. The vapor pressure of Ga is much smaller than that of Sb and Zn. With an increasing x_{Sb}, the Sb vapor pressure increases while the Ga vapor pressure decreases. However, the Zn vapor pressure increases until x_{Sb} reaches approximately 0.2, and then it begins to decrease. The variation trend of the vapor pressure with the fraction of

Table 2 The liquid composition and vapor pressures for the points representing different diffusion systems

	Ga (%)	Sb (%)	Zn (%)	P_{Ga} (atm)	P_{Sb} (atm)	P_{Zn} (atm)	P_{tot} (atm)
P	93.6	3.9	2.5	1.2×10^{-18}	3.6×10^{-18}	5.5×10^{-10}	5.5×10^{-10}
O	16.3	22.7	61.0	2.4×10^{-19}	1.8×10^{-17}	1.0×10^{-8}	1.0×10^{-8}
B	12.9	26.6	60.5	1.9×10^{-19}	2.3×10^{-17}	9.7×10^{-9}	9.7×10^{-9}

Table 3 The ratio of surface concentration and that of effective surface diffusivity between different sources

	Theoretical results	Experimental results
C_{sur} (Zn)/C_{sur} (Zn–Sb)	0.9	1.1
C_{sur} (Zn)/C_{sur} (Zn–Ga)	9.5	8.5
D_{sur} (Zn)/D_{sur} (Zn–Sb)	1.5	1.1
D_{sur} (Zn)/D_{sur} (Zn–Ga)	14.6	12.6

group V element in the liquid phase in Ga/Sb/Zn system is the same as that in Ga/As/Zn system [31]. Table 2 gives the liquid composition and the vapor pressure for the points representing three different diffusion systems. With the values of P_{Sb} and P_{Zn} given in Table 2, one can calculate the ratio of C_{sur} and that of D_{sur} between different sources through Eqs. (23) and (25), as shown in Table 3. The values obtained from the experimental profiles are also given in the table. The word in the parenthesis represents the source composition. As can be seen, C_{sur} (Zn)/C_{sur} (Zn–Sb) and C_{sur} (Zn)/C_{sur} (Zn–Ga) from the theoretical calculations are 0.9 and 9.5, respectively. The corresponding ratios from the experimental profiles are 1.1 and 8.5. The deviations are 22 and 11 %, respectively, which may be attributed to a diffusion time not long enough for the surface concentration to reach an equilibrium value. D_{sur} (Zn)/D_{sur} (Zn–Sb) and D_{sur} (Zn)/D_{sur} (Zn–Ga) from the theoretical calculations are 1.5 and 14.6, respectively. The corresponding ratios by Boltzmann analysis are 1.1 and 12.6. The deviations are 27 and 14 %, respectively. As mentioned above, the Boltzmann–Matano method is not strictly appropriate for our experimental profiles which has not reached a global equilibrium due to the short diffusion time. The agreement between the theoretical and experimental results validates the relationship between the surface diffusion parameters and the vapor pressures as well as the deduced location in the phase diagram for each diffusion system. It can be concluded that compared with the system with sufficient pure Zn source, using sufficient Zn–Sb source moves the liquid phase from point O to point B, resulting in an increase in Sb vapor pressure and a decrease in Zn vapor pressure, the balance of which makes the variation of the surface concentration neglectable. The increase in Sb vapor pressure slightly decreases the effective surface diffusivity, leading to a slight decrease in junction depth, which is not enough to change the shape of the diffusion profile. Instead, using sufficient Zn–Ga source moves the liquid phase from point O to point P, resulting in a decrease of 94.5 % in Zn vapor pressure and a decrease of 80.0 % in Sb vapor pressure, and thus a significantly decreased surface concentration. The decrease of 93.2 % in the effective surface diffusivity leads to a greatly shortened junction depth, which converts the diffusion profile from a kink-and-tail one into a box one.

Conclusion

The experimental results indicated that when the diffusion temperature and time were kept unchanged, the diffusion profiles of Zn in n-GaSb with different sources differ in the surface concentration and effective surface diffusivity. Based on the surface-equilibrium assumption as well as the substitutional–interstitial mechanism, it was deduced that the surface concentration is proportional to the Zn and Sb vapor pressure surrounding the wafer, and that the effective surface diffusivity is inversely proportional to the Sb vapor pressure and proportional to the square of the surface concentration. The Ga/Sb/Zn ternary phase diagram at 500 °C was calculated and each of the experiments was located in this phase diagram, which enabled the calculation of the ambient vapor pressure for each experiment. Thus, the ratio of surface concentration and that of effective surface diffusivity between different sources were calculated, agreeing well with those extracted from

the experimental profiles. The theoretical and experimental results both indicated that, compared with pure Zn source, using Zn–Sb source keeps the surface concentration unchanged but slightly decreases the effective surface diffusivity, while using Zn–Ga source significantly decreases both the surface concentration and effective surface diffusivity.

Acknowledgements

This work was supported by the National Natural Science Foundation of China (Grant No. 51576188).

References

[1] Ikyo AB, Marko IP, Hild K, Adams AR, Arafin S, Amann M-C, Sweeney SJ (2016) Temperature stable mid-infrared GaInAsSb/GaSb vertical cavity surface emitting lasers (VCSELs). Sci Rep 6:19595

[2] Richardson CJ, He L, Apiratikul P, Siwak NP, Leavitt RP (2015) Improved GaSb-based quantum well laser performance through metamorphic growth on GaAs substrates. Appl Phys Lett 106:101108

[3] Peng R, Jiao S, Li H, Zhao L (2015) Dark current mechanisms investigation of surface passivation InAs/GaSb photodiodes at low temperatures. J Alloy Compd 632:575–579

[4] Provence S, Ricker R, Aytac Y, Boggess T, Prineas J (2015) High power cascaded mid-infrared InAs/GaSb light emitting diodes on mismatched GaAs. J Appl Phys 118:123108

[5] Juang B-C, Laghumavarapu RB, Foggo BJ, Simmonds PJ, Lin A, Liang B, Huffaker DL (2015) GaSb thermophotovoltaic cells grown on GaAs by molecular beam epitaxy using interfacial misfit arrays. Appl Phys Lett 106:111101

[6] Wang Y, Chen N, Zhang X, Huang T, Yin Z, Wang Y, Zhang H (2010) Evaluation of thermal radiation dependent performance of GaSb thermophotovoltaic cell based on an analytical absorption coefficient model. Sol Energy Mater Sol Cells 94:1704–1710

[7] Cunha SFD, Bougnot J (1974) Diffusion and solubility of Zn in GaSb. Phys Status Solidi 22:205–208

[8] Sundaram VS, Gruenbaum PE (1993) Zinc diffusion in GaSb. J Appl Phys 73:3787–3789

[9] Conibeer GJ, Willoughby AFW, Hardingham CM, Sharma VKM (1996) Zinc diffusion in tellurium doped gallium antimonide. J Electron Mater 25:1108–1112

[10] Bett AW, Keser S, Sulima OV (1997) Study of Zn diffusion into GaSb from the vapour and liquid phase. J Cryst Growth 181:9–16

[11] Mimkes J, Šestáková V, Nassr K, Lübbers M, Štěpánek B (1998) Diffusion mobility and defect analysis in GaSb. J Cryst Growth 187:355–362

[12] Nicols SP, Bracht H, Benamara M, Liliental-Weber Z, Haller EE (2001) Mechanism of zinc diffusion in gallium antimonide. Phys B 308:854–857

[13] Sulima OV, Bett AW, Mauk MG, Ber BY, Dutta PS (2003) Diffusion of Zn in TPV materials: GaSb, InGaSb, InGaAsSb and InAsSbP. In: 5th conference on thermophotovoltaic generation of electricity, AIP Publishing, Melville, pp. 402–413

[14] Schlegl T, Sulima O, Bett A (2004) The influence of surface preparation on Zn-diffusion processes in GaSb. In: 6th conference on thermophotovoltaic generation of electricity, AIP Publishing, Melville, pp. 396–403

[15] Sunder K, Bracht H, Nicols SP, Haller EE (2007) Zinc and gallium diffusion in gallium antimonide. Phys Rev B 75:245210

[16] Ye H, Tang LL, Ma YL (2010) Experimental and theoretical investigation of zinc diffusion in n-GaSb. Chin Sci Bull 55:2489–2496

[17] Ye H, Tang LL, Li KJ (2013) The intrinsic relationship between the kink-and-tail and box-shaped zinc diffusion profiles in n-GaSb. Semicond Sci Technol 28:015001

[18] Tuck B, Jay PR (1976) Application of the phase diagram to the diffusion of Zn in GaP. J Phys D 9:2225

[19] Hettwer H-G, Stolwijk NA, Mehrer H (1997) Effects of source composition on diffusion and solubility of zinc in gallium arsenide. Defect Diffus Forum 143:1117–1124

[20] Tuck B, Hooper A (1975) Diffusion profiles of zinc in indium phosphide. J Phys D 8:1806

[21] Hooper A, Tuck B, Baker AJ (1974) Diffusion of zinc in indium phosphide at 700 °C. Solid-State Electron 17:531–538

[22] Serreze HB, Marek HS (1986) Zn diffusion in InP: effect of substrate dopant concentration. Appl Phys Lett 49:210–211

[23] Longini RL (1962) Rapid zinc diffusion in gallium arsenide. Solid-State Electron 5:127–130

[24] Gösele U, Morehead F (1981) Diffusion of zinc in gallium arsenide: a new model. J Appl Phys 52:4617–4619

[25] Ting CH, Pearson GL (1971) Time-dependence of zinc diffusion in gallium arsenide under a concentration gradient. J Electrochem Soc 118:1454–1458

[26] Tuck B, Kadhim MAH (1972) Anomalous diffusion profiles of zinc in GaAs. J Mater Sci 7:585–591

[27] Shih K, Allen J, Pearson G (1968) Diffusion of zinc in gallium arsenide under excess arsenic pressure. J Phys Chem Solids 29:379–386

[28] Jäger W, Rucki A, Urban K, Hettwer HG, Stolwijk N, Mehrer H, Tan T (1993) Formation of void/Ga-precipitate

pairs during Zn diffusion into GaAs: the competition of two thermodynamic driving forces. J Appl Phys 74:4409–4422

[29] Liu EK, Zhu BS, Luo JS (2011) The physics of semiconductor, 7th edn. Electron Industry, Beijing

[30] Dervišević I, Todorović A, Talijan N, Djokic J (2010) Experimental investigation and thermodynamic calculation of the Ga–Sb–Zn phase diagram. J Mater Sci 45:2725–2731

[31] Panish MB (1966) The gallium-arsenic-zinc system. J Phys Chem Solids 27:291–298